NJC

Accepted Manuscript

This article can be cited before page numbers have been issued, to do this please use: R. Saito, M. Tamura, S. Kawano, Y. Yoshikawa, A. Kato, K. SASAKI and H. Yasui, *New J. Chem.*, 2017, DOI: 10.1039/C7NJ00970D.

ROYAL SOCIETY OF CHEMISTRY

rsc.li/njc

NJC

View Article Online
DOI: 10.1039/C7NJ00970D

ARTICLE

Synthesis and biological evaluation of 4-hydroxy-5-oxo-2,5-dihydro-1*H*-pyrrole-3-carboxamides and their zinc(II) complexes as candidate antidiabetic agents

Received 00th January 20xx,
Accepted 00th January 20xx

DOI: 10.1039/x0xx00000x

www.rsc.org/

Ryota Saito,*[a,b] Moe Tamura,[a] Saya Kawano,[a] Yutaka Yoshikawa,[c] Akihiro Kato,[a] Kaname Sasaki,[a] and Hiroyuki Yasui[d]

The newly designed 1-(arylmethyl)-2,5-dihydro-4-hydroxy-5-oxo-1*H*-pyrrole-3-carboxamides (**1a–e**) were synthesized by using *N*-tritylated acrylamide as a starting material, and their zinc(II) complexes (**10a–e**) were readily prepared by simply mixing **1a–e** and $ZnSO_4$ in the presence of LiOH. Aldose reductase (AR) inhibitory activity of **1a–e** were evaluated to reveal important structural features for 2,5-dihydro-5-oxo-1*H*-pyrrole derivatives to exhibit high AR inhibitory activity. The *in vitro* insulin–mimetic activity of these complexes was evaluated from 50% inhibitory concentrations (IC_{50}) on free fatty acid (FFA) release from isolated rat adipocytes treated with epinephrine. Four out of the five newly synthesized complexes exhibited higher *in vitro* insulin-mimetic activities than $ZnSO_4$, a positive control. This study proved that the newly synthesized N_2O_2-coordination-type zinc(II) complexes based on pyrrole-3-carboxamide derivatives (**1a–d)** are potential hypoglycemic agents.

Introduction

Diabetes is characterized as a state of chronic hyperglycemia that is caused by a decrease in the level and/or function of insulin, which is a peptide hormone secreted by the β cells of the pancreatic islets of Langerhans to regulate the blood glucose level.[1] Diabetes is generally categorized into type 1 and type 2,[2] where type 2 diabetes patients comprise more than 90% of all diabetes patients.[3]

Type 1 diabetes results from an absolute shortage of insulin, caused by destruction of the pancreatic β cells, autoimmune insulitis, or other related conditions, and hence it is not a lifestyle-related disease.[2] Type 1 diabetes develops in childhood or early adulthood and, to date, the only available treatment involves direct administration of insulin as insulin injections, which generally lead to physical and emotional distress in diabetes patients. In contrast, type 2 diabetes is a lifestyle-related disease, caused by obesity, stress, insufficient exercise, and aging.[2] These factors can result in insufficient secretion and impaired action of insulin. Primary treatments of type 2 diabetes involve exercise and diet management without pharmacotherapeutic intervention. When these methods become ineffective, administration of synthetic hypoglycemic agents, such as sulfonylureas, meglitinides, and biguanides, is initiated.[4] However, some oral antidiabetic agents exhibit side effects, including hypoglycemia, nausea, and convulsions.[4] In addition, continuous repression of the blood glucose levels using pharmacotherapy can be misinterpreted by the body that it no longer needs to synthesize insulin and thus, it quits synthesizing the peptide, eventually forcing the patients to rely on exogenous insulin injections.[4]

In addition, diabetes can lead to serious complications, including neuropathy, retinopathy and nephropathy.[2] The onset of the complications is the most critical aspect for diabetics, and is strongly related to the polyol metabolic pathway. Under the circumstances of hyperglycemia, the amount of glucose taken up into the cells increases and glucose overflows from the normal glycolytic pathway into the polyol metabolic pathway to consume the excess glucose.[5, 6] During the first step of the polyol metabolic pathway, glucose is reduced to sorbitol by aldose reductase (AR) using NADPH as a coenzyme and then, the resulting sorbitol is oxidized to fructose (Fig. 1).[5, 6] Because the second step is slower than the first one, sorbitol abnormally accumulates in the cells, accompanied by excessive consumption of NADPH. This state increases the intracellular osmolality, inhibits the uptake of important molecules and ions into the cell, and eventually causes macular edema. In addition, excessive consumption of NADPH hinders the other pathways that utilize NADPH as a coenzyme, leading to increased oxidative stress that results in various complications.[5, 7] Thus, inhibition of AR, involved in the first step of the pathway, is considered essential to prevent the onset or progression of diabetes complications.[8, 9] Based on these findings, it is highly desirable to develop new antidiabetic agents, which not only replace the subcutaneous insulin injections and the oral hypoglycemic drugs but also simultaneously inhibit AR to decrease the risk of diabetes complications.

[a] Department of Chemistry, Toho University, 2-2-1 Miyama, Funabashi, Chiba, 274-8510 Japan. E-mail: saito@chem.sci.toho-u.ac.jp
[b] Research Center for Materials with Integrated Properties, Toho University, 2-2-1 Miyama, Funabashi, Chiba 274-8510, Japan.
[c] Department of Health, Sports and Nutrition, Kobe Women's University, 4-7-2 Minatojima-nakamachi, Chuo-ku, Kobe 650-0046, Japan
[d] Department of Analytical and Bioinorganic Chemistry, Kyoto Pharmaceutical University, Kyoto 607-8414, Japan.

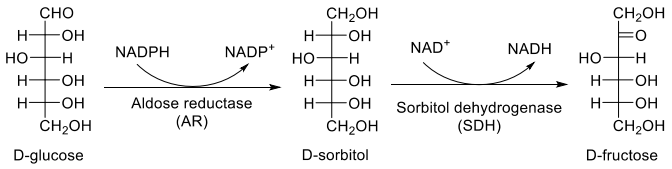

Fig. 1 Schematic presentation of the polyol pathway of glucose metabolism.

Zinc(II) ion has received considerable attention by medicinal chemists as a new diabetic agent since the insulin-mimetic activity of zinc(II) ion was discovered by Coulston *et al*. in 1980.[10] Numerous studies have been conducted during the last two decades to develop new oral antidiabetic drugs based on zinc(II) ion. For instance, oral administration of $ZnCl_2$ to streptozotocin-induced diabetic rats could decrease the high blood glucose levels,[11, 12] and zinc oxide nanoparticles improved insulin levels in diabetic rats.[13] Despite the promising potency, the inorganic form of zinc(II) is poorly absorbed; this feature necessitates higher dosages, which subsequently increase the adverse drug reactions.[10, 13] Thus, organic zinc(II) compounds were used, which, in addition, exhibited enhanced therapeutic effects.[10] Thereafter, many zinc(II) complexes have been developed and showed insulin-mimetic activity both *in vitro* and *in vivo*.[10, 14-21]

Recently, we have synthesized zinc(II) complexes using ethyl 1-benzyl-4-hydroxy-5-oxo-2,5-dihydro-1*H*-pyrrole-3-carboxylate (EBPC, Fig. 2) and its derivatives as organic ligands. We showed, for the first time, that they exhibited insulin-mimetic activities.[22] In addition, the ligands themselves have AR inhibitory activity;[23] thereby the complexes are potential bifunctional chemotherapeutics for both diabetes and its complications. The coordination mode of the EBPCs toward the central zinc(II) ion was determined by means of X-ray crystallographic analysis, which showed that the complex had a planar *trans*-conformation, where the zinc(II) ion was configured with the hydroxyl oxygen at the C3 and the ester carbonyl oxygen at the C4 of the EBPCs.[22] It is known that the coordination mode of the ligands toward zinc(II) affects their bioavailability and therapeutic potency.[10,24] However, only the $Zn(O_4)$ coordination mode has been investigated regarding the Zn-EBPC system. Thus, in the present study, which is a part of our ongoing project on the development of chemotherapeutics based on the zinc(II) complexes of the EBPC derivatives, we synthesized several new zinc(II) complexes, with $Zn(N_2O_2)$ coordination mode, using the new 4-hydroxy-5-oxo-2,5-dihydro-1*H*-pyrrole-3-carboxamide derivatives as ligands. In addition, we evaluated their insulin-mimetic activities to investigate whether replacing the oxygen atoms of the EBPCs by nitrogen atoms affected their insulin-mimetic activity or not. The *in vitro* AR inhibitory activity of the new ligands was also investigated.

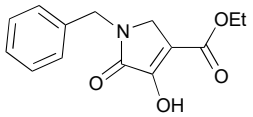

Fig. 2 Structure of ethyl 1-benzyl-4-hydroxy-5-oxo-2,5-dihydro-1*H*-pyrrole-3-carboxylate (EBPC).

View Article Online
DOI: 10.1039/C7NJ00970D

Results and Discussion

Synthesis

First, we synthesized **1a**–**e**, the corresponding conjugate acids of the ligands in the target zinc(II) complexes, using the same reaction scheme as that used for synthesizing EBPC and its derivatives.[22] Briefly, conjugate addition of the benzyl amines, **4a**–**e**, toward acrylamide was conducted and the corresponding conjugate adducts, **5a**–**e**, were obtained in good yield. The conjugate adducts, **5a**–**e**, were sequentially reacted with diethyl oxalate in the presence of sodium ethoxide (Scheme 1). When **5a** was subjected to the reaction, the target amide, **1a**, was obtained accompanied by the formation of the ester, **6a**. The ratio of **1a**:**6a** was determined as 1.3:1 by ^{1}H-NMR spectroscopy. Similar amide-ester transformations occurred with **5b**–**e**. Although determination of the product ratio and purification of the esters were not fulfilled, it is obvious that this side reaction decreased the yields of the desired amides, **1b**–**e**.

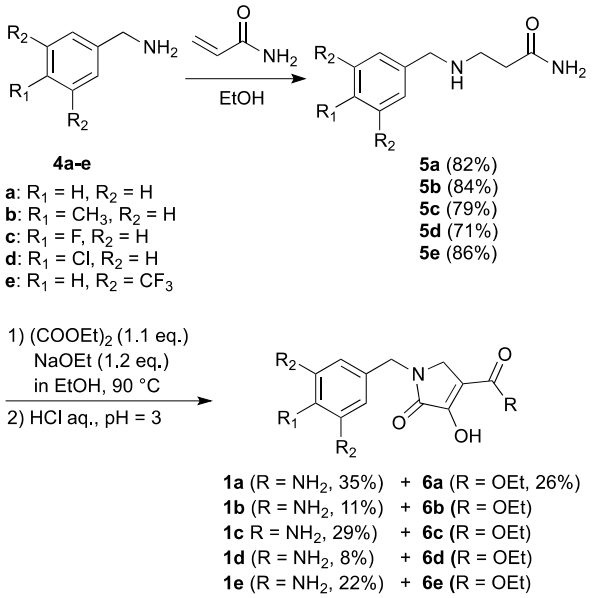

Scheme 1 Synthetic route to amides **1a**–**e** accompanied by undesired amide-ester transformation products.

This amide-ester transformation reaction was first considered to occur when the surplus ethoxide attacks the amide carbonyl carbon of the product. Thus, we carried out the same reaction using 0.94 equivalent of sodium ethoxide (Scheme 2, eq.1). However, ester formation was still observed. We also investigated the effect of the reaction temperature on the amide-ester transformation reaction. It was found that lowering the reaction temperature resulted in not only a diminished yield of the amide but also formation of the ester (Scheme 2, eq.2). These results suggested that the excess amount of the base and the reaction temperature did not influence the occurrence of this side reaction.

View Article Online
DOI: 10.1039/C7NJ00970D

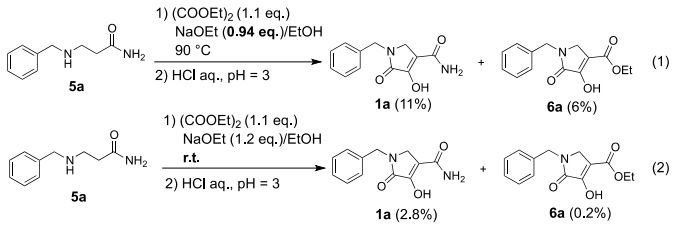

Scheme 2 Reaction of amide **5a** with diethyl oxalate under various conditions.

In order to investigate whether the amide groups in the starting materials of the cyclocondensation reaction and the produced amides incur the amide-ester transformation reaction with sodium ethoxide or not, **5a** and **1a** were sequentially treated with sodium ethoxide under the same conditions used for the cyclocondensation reaction in Scheme 1 (Scheme 3). It was found that the amides remained intact under these conditions, which indicated that the amide-ester transformation reaction did not proceed at the initial and final stages of the cyclocondensation reaction (Scheme 3).

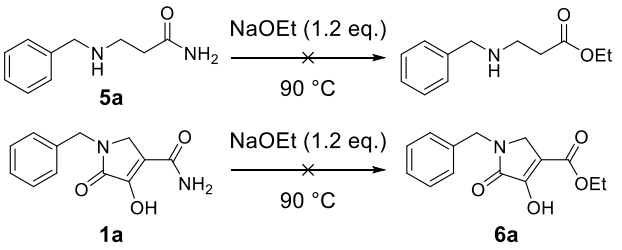

Scheme 3 Examination of the reactivity of amides **1a** and **5a** with sodium ethoxide.

Based on these results, we suggested a different reaction mechanism for the amide-ester transformation, as illustrated in Scheme 4, which involves the generation of a pyrrolidinetrione intermediate (**A**) during the course of the reaction followed by opening of the cyclic imide *via* the attack of ethoxide, and subsequent cyclocondensation to form the amide-ester transformation product.

Assuming that the amide-ester transformation reaction occurs *via* this mechanism, bulking of the terminal amide is considered to prevent the imide formation and consequently suppress the amide-ester transformation reaction. Thus, we used a new synthetic route, in which the *N*-tritylacrylamide, **7**,[25] was employed as a Michael acceptor (Scheme 5). The reaction of **7** with benzylamines **4a**–**e** gave the corresponding **8a**–**e**, which were subsequently reacted with diethyl oxalate in the presence of sodium ethoxide to provide **9a**–**e** in moderate to good yields. It should be emphasized that no amide-ester transformation product was observed. These results obviously supported the suggested mechanism in Scheme 4. Compounds **9a**–**e** were detritylated under acidic conditions to obtain the desired products, **1a**–**e**, in satisfactory yields.

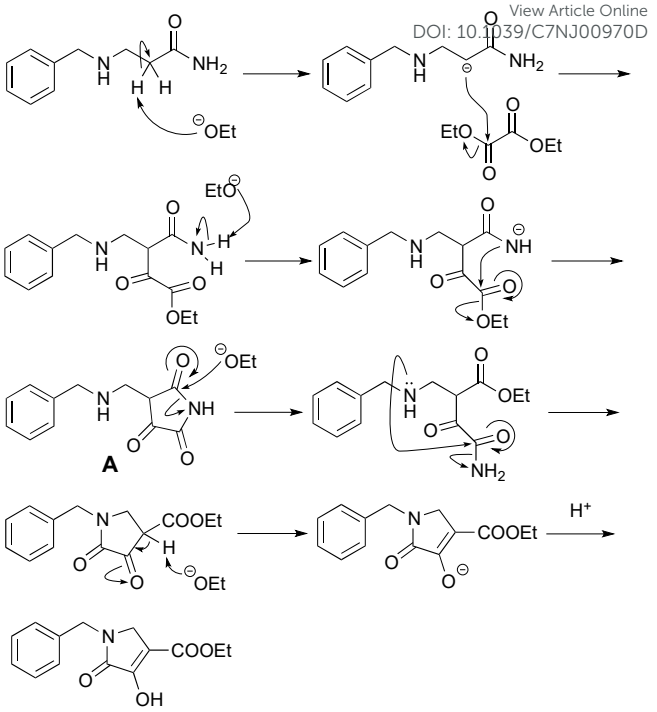

Scheme 4 Proposed reaction mechanism for the amide-ester transformation during the synthesis of **1**.

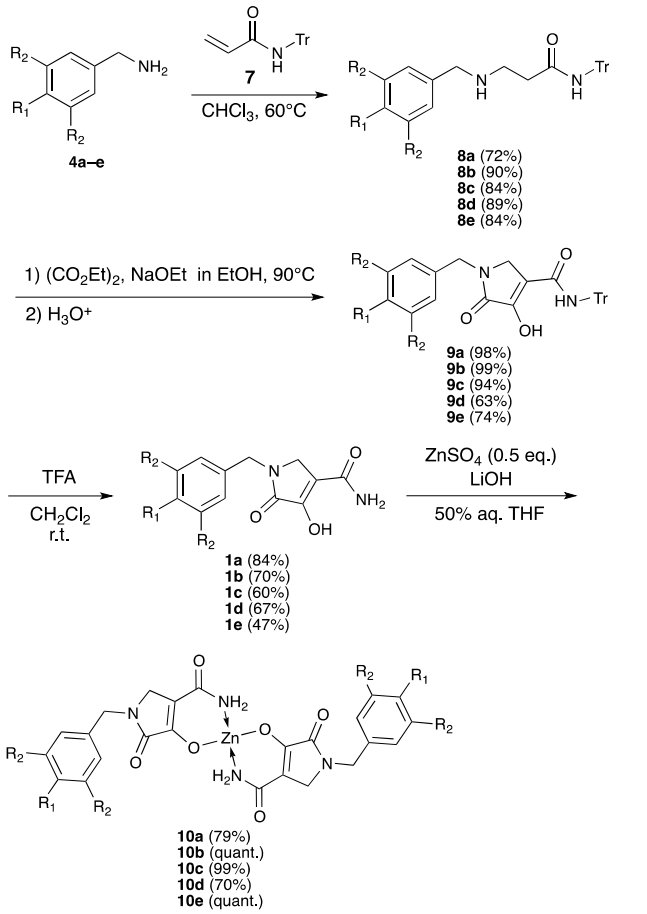

Scheme 5 Improved synthetic route to zinc(II) complexes **10a**–**e**.

View Article Online
DOI: 10.1039/C7NJ00970D

Then, **1a**–**e** were reacted with zinc sulfate in the presence of lithium hydroxide to afford the corresponding zinc(II) complexes, **10a**–**e** (Scheme 5). In all cases, the reactions provided the desired products in good yields. The structures of the complexes were assigned on the basis of their spectroscopic data and combustion analysis. In ^{1}H-NMR spectra, each ligand showed two broad peaks around 7 ppm, assignable to the non-equivalent amide NH protons, while these signals disappeared on complexation with zinc(II) ion, as exemplified by the spectra for **1b** (Fig. 3). Some zinc(II)-amide complexes with the amide carbonyl oxygens coordinating with zinc(II) ion showed discernible signals for the amide NH protons in their ^{1}H-NMR spectra.[26, 27] Based on these facts, the coordination mode of the ligands in **10a**–**e** was determined as that the zinc(II) ion was configured with the amide nitrogen and the hydroxide oxygen at C3 position as depicted in Scheme 5.

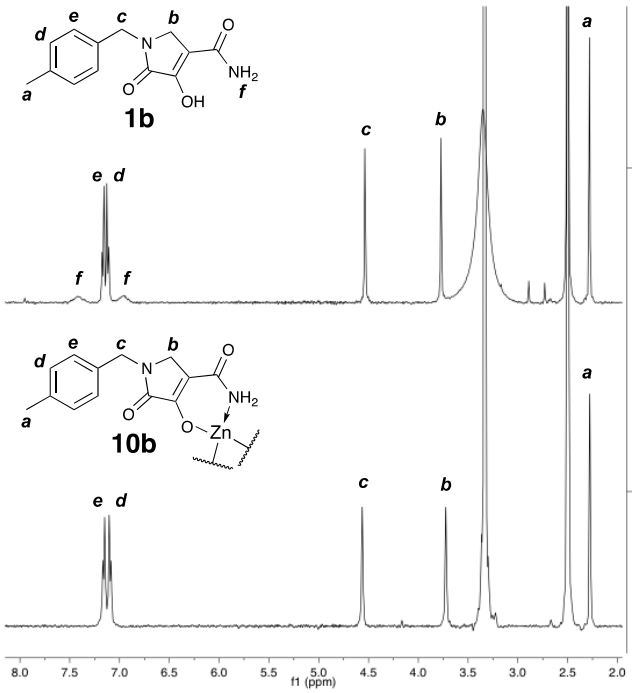

Fig. 3 ^{1}H NMR spectra (400 MHz at 25 °C in DMSO-d_6) of selected **1b** and its zinc(II) complex **10b**.

***In vitro* aldose reductase inhibitory activities of 1a–e**

The AR inhibitory activities of **1a**–**e** were evaluated *in vitro via* measurement of their inhibitory effects on the reduction of D,L-glyceraldehyde, which was catalyzed by recombinant human AR in the presence of NADPH as a cofactor.[28] The assays were based on spectrophotometric monitoring of NADPH consumption, which was proven a reliable method.[29] The results are presented in Table 1.

Compounds **1a**–**e** showed 16–28% inhibition at a concentration of 30 μM, thus their half maximal inhibitory concentration (IC_{50}) values were not determined owing to their low efficacy. These compounds were expected to exhibit the same inhibitory activity as that of EBPC because they possess the hydroxyl group at the C4-position, which was considered crucial for a high AR inhibitory activity[23], whereas the ester group at C3 was not expected to affect the activity. However, their AR inhibitory activity was greatly decreased compared to that of EBPC. Based on these findings, we suggested that not only the 4-hydroxyl group but also the ester moiety at the 3-position was essential for the high AR inhibitory activity of the 2,5-dihydro-5-oxo-1*H*-pyrrole derivatives.

Table 1. The *in vitro* AR inhibitory activities of **1a**–**e**

Compounds		R_1	R_2	Inhibition rate
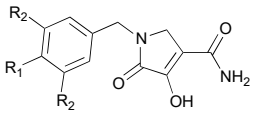	**1a**	H	H	16% at 30 μM
	1b	CH_3	H	17% at 30 μM
	1c	F	H	23% at 32 μM
	1d	Cl	H	26% at 31 μM
	1e	H	CF_3	28% at 31 μM
epalrestat[a]		-	-	50% at 0.066 μM
EBPC		-	-	50% at 0.20 μM

[a]Epalrestat was used as a reference compound.

In order to better interpret these findings, molecular docking simulations of EBPC and **1a** in the active site of the enzyme were performed. In these experiments, the protein structure coded as 2FZD in the Protein Data Bank (PDB) was employed because this protein structure has been frequently used in the docking studies of the AR inhibitors.[30-33] The results of molecular docking are depicted in Fig. 4. EBPC was predicted to interact with His110 and Trp111, which form the active site of AR together with Tyr48, *via* formation of hydrogen bonds with the hydroxide anion at C4 and with the 5-oxo moiety, respectively, besides the interaction of the carbonyl oxygen of the ester group with Trp20, present in the vicinity of the active site (Fig. 4a). The active site of AR is frequently called an "anion-binding pocket" because His110 is positively charged at physiological pH and therefore attracts the negatively charged substituents.[34] Hence, the predicted docking pose well explained the high AR inhibitory activity of EBPC. On the contrary, compound **1a** formed hydrogen bonds with His110 and $NADP^+$ through the C3-carboxamide moiety, whereas the anionic substituent at C4 was left out of the anion-binding active site (Fig. 4b). This suggested that the binding of **1a** to the active site was weaker than that of EBPC, which rationally explained the observed decrease in the AR inhibitory effects.

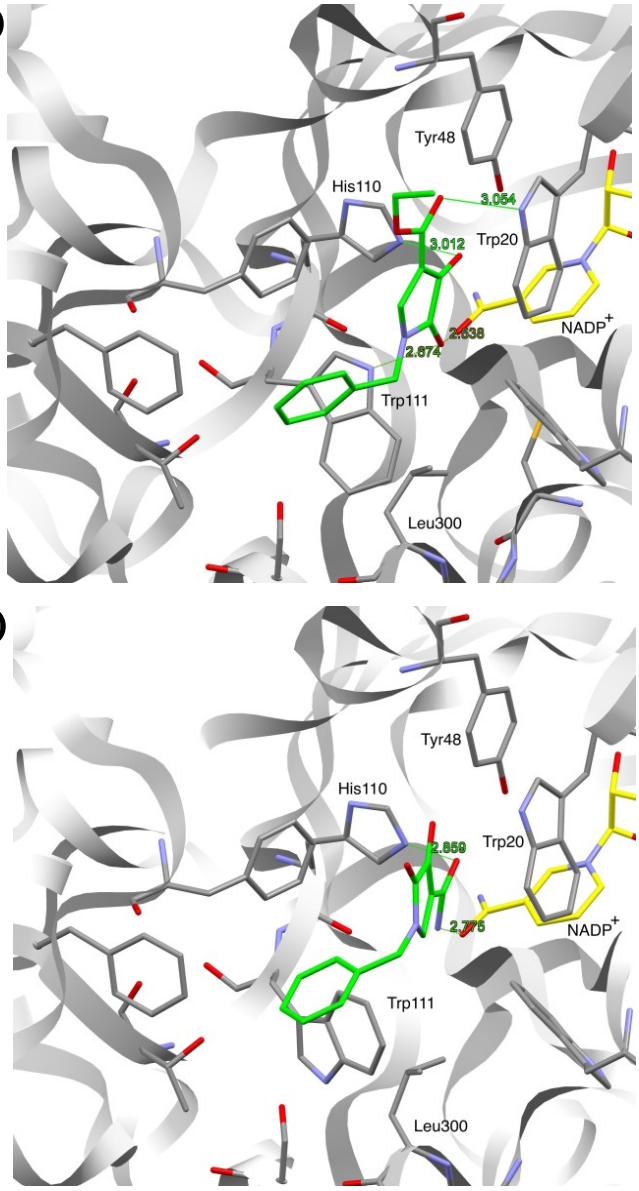

Fig. 4 Depiction of the predicted docking poses for (a) EBPC and (b) **1a** in the active site of 2FZD. The inhibitors are depicted in green, and $NADP^+$ in yellow.

Evaluation of the insulin-mimetic activity of the zinc(II) complexes

To evaluate the insulin-mimetic activity of the synthesized zinc(II) complexes (**10a**–**e**) *in vitro*, we investigated the inhibitory effects of the complexes on free fatty acid (FFA) release from rat adipose cells stimulated with epinephrine. This method was proven simple and reliable.[14, 22, 35] As shown in Fig. 4, all complexes, except **10e,** inhibited the FFA release in a dose-dependent manner, which showed that complexes **10a**–**d** exhibited insulin-mimetic activity. Compound **10e** was hardly soluble in the assay medium, therefore, its inhibitory activity could not be determined. The quantitative evaluation of the inhibitory activity of **10a**–**d** was carried out *via* calculation of the IC_{50} value, which was defined as the concentration of the complex that resulted in 50% inhibition of the FFA release. The results of the assay are summarized in Table 2. All the complexes, **10a–d**, exhibited a slightly greater activity than zinc sulfate, which was used as a positive control.

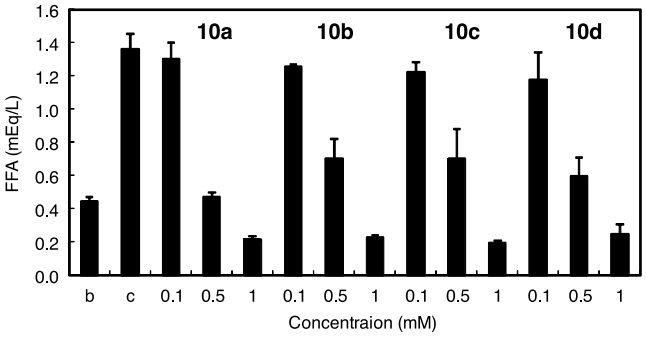

Fig. 5 The inhibitory effects of zinc(II) complexes, **10a–d,** on epinephrine-stimulated FFA release from rat adipocytes. The letter "b" stands for "blank" and "c" for "control."

Moreover, the activities of the studied complexes were the same as those of the previously investigated zinc(II) complexes based on EBPC (0.26–0.82 mM).[22] Regarding the coordination mode of the ligands toward zinc(II) ion, no significant differences were observed between the IC_{50} values of the studied complexes and those of the previously investigated zinc(II) complexes with the corresponding esters. The present complexes exhibited higher activity than $ZnSO_4$, thereby they are potential candidates for hypoglycemic agents.

Table 2. The *in vitro* insulin-mimetic activities of **10a**–**d**

Zn complex	IC_{50} (mM)
10a	0.37
10b	0.36
10c	0.39
10d	0.41
$ZnSO_4$	0.44[†]

[†] Data was taken from reference 17

Conclusions

To synthesize the 2,5-dihydro-4-hydroxy-5-oxo-1*H*-pyrrole-3-carboxamide derivatives (**1a**–**e**), the problem of amide-ester transformation during the cyclocondensation step was encountered. After careful examination, we figured out the cause and mechanism of the amide-ester transformation reaction. We were able to effectively obtain the desired amides using an appropriate protecting group. This could help the future synthesis of the series of the 2,5-dihydro-4-hydroxy-5-oxo-1*H*-pyrrole derivatives. All the newly synthesized complexes with $Zn(N_2O_2)$ coordination mode demonstrated a sufficient insulin-mimetic activity that allows their probable classification as hypoglycemic agents because their IC_{50} values were slightly higher than that of $ZnSO_4$ and comparable to those of the corresponding $Zn(O_4)$-type complexes based on the EBPC derivatives. These results provided useful information about the structure-activity relationship of zinc(II) complexes based on

2,5-dihydro-4-hydroxy-5-oxo-1*H*-pyrrole derivatives, which could aid the development of new chemotherapeutics for treating diabetes.

Acknowledgements

This research was supported by JSPS KAKENHI Grant Number JP25410179. The partial financial support to RS by the MEXT-Supported Program for the Strategic Research Foundation at Private Universities at Toho University, 2012-2016 (S1201034), is gratefully appreciated. YY and HY were financially supported, in part, by a grant from the MEXT-Supported Program for the Strategic Research Foundation at Private Universities at Kyoto Pharmaceutical University, 2012-2016 (S1201008). The authors would like to thank Editage (www.editage.jp) for English language editing.

Experimental

General

^{1}H-NMR spectra were recorded using an ECP-400 spectrometer (JEOL Ltd., Japan). Chemical shifts (δ) are expressed in ppm employing tetramethylsilane (TMS) or a non-deuterated solvent as internal standards in the deuterated solvent used. Coupling constants (*J*) were given in Hz. ^{13}C-NMR spectra were recorded using the ECP-400 spectrometer (JEOL Ltd., Japan). Chemical shift multiplicities were expressed as s = singlet, d = doublet, t = triplet, q = quintet, m = multiplet. Infrared (IR) spectra were obtained using FT/IR-4100, FT/IR-660 plus, or FT/IR-460 plus spectrophotometers (JASCO., Ltd, Japan). Fast-atom bombardment (FAB) mass spectra were recorded using a JMS-600-H mass spectrometer (JEOL Ltd., Japan). Xenon was used as a bombardment gas, and all analyses were carried out in a positive ion mode with the ionization energy and accelerating voltage set at 70 eV and 3 kV, respectively. A mixture of dithiothreitol (DTT) and α-thioglycerol (TG) (1:1) was used as a liquid matrix.

All conventional chemicals used in the present study are commercially available and were used as received. Column chromatography was carried out on silica gel (particle size, 46–50 µm; Fuji Silysia Chemical Ltd., Japan). Recombinant human aldose reductase (AR), produced by ATGen Co., Ltd., was purchased from Cosmo Bio Co., Ltd.

Synthesis

*3-(Benzylamino)-N-tritylpropanamide (**8a**)*

Benzylamine (160 µl, 1.46 µmol) was added dropwise to *N*-trithylacrylamide (309 mg, 985 µmol) in chloroform (4 ml) at r.t., and then the mixture was stirred at 60 °C for 2 days. After evaporation of the solvent, the obtained yellow solid was purified by column chromatography on silica gel (46–50 µm, hexane:ethyl acetate = 9:1, chloroform:ethyl acetate = 1;1) to afford the product as light yellow solid (299 mg, 72%). Mp 168.0–168.9 °C. ^{1}H NMR (400 MHz, $CDCl_3$) δ/ppm 2.40–2.4 (m, 2H), 2.91–2.97 (m, 2H), 3.74 (s, 2H), 7.04–7.09 (m, 2H), 7.19–7.28 (m, 18H), 9.32 (s, 1H). ^{13}C NMR (100 MHz, $CDCl_3$) δ/ppm 36.7, 45.4, 54.0, 70.3, 126.9, 127.3, 128.0, 128.4, 128.7, 128.9, 139.2, 145.2, 171.7. IR (KBr) ν_{max}/cm^{-1} 3455 (νN-H), 3275 (νN-H), 3024–2853 (νC-H), 1664 (νC=O), 1551 (δN-H). MS (FAB$^+$, DTT/TG = 1/1) m/z 421 [M+H]$^+$. HRMS (positive ESI) Calcd for $C_{29}H_{29}N_2O^+$ [M+H]$^+$: 421.2274. Found: 421.2296.

View Article Online DOI: 10.1039/C7NJ00970D

*3-((4-Methylbenzyl)amino)-N-tritylpropanamide (**8b**)*

4-Methylbenzylamine (600 µl, 4.75 mmol) was added dropwise to *N*-trithylacrylamide (1.01 g, 3.21 mmol) in chloroform (12 ml) at r.t., and then the mixture was stirred at 60 °C for 2 days. After evaporation of the solvent, the obtained yellow solid was purified by column chromatography on silica gel (46–50 µm, chloroform:ethyl acetate = 4:1, 1;1) to afford the product as light yellow solid (1.26 g, 90%). Mp 159.5–160.0 °C. ^{1}H NMR (400 MHz, $CDCl_3$) δ/ppm 2.34 (s, 3H), 2.39–2.44 (m, 2H), 2.91–2.96 (m, 2H), 3.72 (s, 2H), 6.95 (d, *J* = 7.7 Hz, 2H), 7.04 (d, *J* = 7.7 Hz, 2H), 7.18–7.29 (m, 15H), 9.42 (s, 1H). ^{13}C NMR (100 MHz, $CDCl_3$) δ/ppm 21.2, 36.9, 45.3, 53.7, 70.3, 126.9, 127.9, 128.3, 128.9, 129.3, 136.2, 136.9, 145.3, 171.8. IR (KBr) ν_{max}/cm^{-1} 3455 (νN-H), 3240 (νN-H), 3060–2826 (νC-H), 1644 (νC=O), 1531 (δN-H). MS (FAB$^+$, DTT/TG = 1/1) m/z 435 [M+H]$^+$. HRMS (positive ESI) Calcd for $C_{30}H_{31}N_2O^+$ [M+H]$^+$: 435.2431. Found: 435.2412.

*3-((4-Fluorobenzyl)amino)-N-tritylpropanamide (**8c**)*

4-Fluorobenzylamine (600 µl, 4.84 mmol) was added dropwise to *N*-trithylacrylamide (1.04 g, 3.33 mmol) in chloroform (12 ml) at r.t., and then the mixture was stirred at 60 °C for 3 days. After evaporation of the solvent, the obtained yellow solid was purified by column chromatography on silica gel (46–50 µm, chloroform:ethyl acetate = 4:1, 1;1) to afford the product as colorless solid (1.22 g, 84%). Mp 173.8–174.0 °C. ^{1}H NMR (400 MHz, $CDCl_3$) δ/ppm 2.40–2.46 (m, 2H), 2.89–2.96 (m, 2H), 3.72 (s, 2H), 6.89 (t, *J* = 8.7, 2H), 6.96–7.03 (m, 2H), 7.17–7.29 (m, 15H), 9.14 (s, 1H). ^{13}C NMR (100 MHz, $CDCl_3$) δ/ppm 36.9, 45.3, 53.3, 70.4, 115.4 (d, $^2J_{CF}$ = 21 HZ), 127.0, 128.0, 128.9, 129.9 (d, $^3J_{CF}$ = 8 HZ), 135.0, 145.2, 162.1 (d, $^1J_{CF}$ = 246 HZ), 171.6. IR (KBr) ν_{max}/cm^{-1} 3474 (νN-H), 3267 (νN-H), 3145–2901 (νC-H), 1660 (νC=O), 1545 (δN-H), 1218 (νC-F). MS (FAB$^+$, DTT/TG = 1/1) m/z 439 [M+H]$^+$. HRMS (positive ESI) Calcd for $C_{29}H_{28}FN_2O^+$ [M+H]$^+$: 439.2180. Found: 439.2161.

*3-((4-Chlorobenzyl)amino)-N-tritylpropanamide (**8d**)*

4-Cholorobenzylamine (300 µl, 2.45 mmol) was added dropwise to *N*-trithylacrylamide (501 mg, 1.60 mmol) in chloroform (3 ml) at r.t., and then the mixture was stirred at 60 °C for 2 days. After evaporation of the solvent, the obtained yellow solid was purified by column chromatography on silica gel (46–50 µm, chloroform:ethyl acetate = 1;1) to afford the product as colorless solid (645 mg, 89%). Mp 177.0–177.5 °C. ^{1}H NMR (400 MHz, $CDCl_3$) δ/ppm 2.40–2.45 (m, 2H), 2.89–2.95 (m, 2H), 3.72 (s, 2H), 6.97 (d, *J* = 8.2 Hz, 2H), 7.14–7.31 (m, 17H), 9.06 (s, 1H). ^{13}C NMR (100 MHz, $CDCl_3$) δ/ppm 37.0, 45.3, 53.3, 70.4, 127.0, 128.0, 128.7, 128.9, 129.7, 133.0, 137.8, 145.1, 171.4. IR (KBr) ν_{max}/cm^{-1} 3446 (νN-H), 3244 (νN-H), 3030–2828 (νC-H), 1643 (νC=O), 1530 (δN-H). MS (FAB$^+$, DTT/TG = 1/1) m/z 455 [M+H]$^+$. HRMS (positive ESI) Calcd for $C_{29}H_{28}ClN_2O^+$ [M+H]$^+$: 455.1885. Found: 455.1871.

View Article Online
DOI: 10.1039/C7NJ00970D

*3-((3,5-Bis(trifluoromethyl)benzyl)amino)-N-tritylpropanamide (**8e**)*

3,5-Bis(trifluoromethyl)benzylamine (583 mg, 2.40 mmol) was added dropwise to *N*-trithylacrylamide (501 mg, 1.60 mmol) in chloroform (3 ml) at r.t., and then the mixture was stirred at 60 °C for 9 days. After evaporation of the solvent, the obtained yellow solid was purified by column chromatography on silica gel (46–50 μm, chloroform:ethyl acetate = 1;1) to afford the product as colorless solid (747 mg, 84%). Mp 143.0–144.0 °C. ^{1}H NMR (400 MHz, $CDCl_3$) δ/ppm 2.47–2.52 (m, 2H), 2.92–2.97 (m, 2H), 3.86 (s, 2H), 3.98 (s, 1H), 7.18–7.29 (s, 15H), 7.69 (s, 2H), 7.77 (s, 1H), 7.89 (s, 1H). ^{13}C NMR (100 MHz, $CDCl_3$) δ/ppm 37.1, 45.5, 53.2, 70.6, 121.3 (q, $^3J_{CF}$ = 4 HZ), 123.4 (q, $^1J_{CF}$ = 274 HZ), 127.1, 128.0, 128.2 (q, $^3J_{CF}$ = 4 HZ), 128.7 131.8 (q, $^2J_{CF}$ = 33 HZ), 142.4, 144.9, 171.1. IR (KBr) ν_{max}/cm^{-1} 3438 (νN-H), 3240 (νN-H), 2849-3029 (νC-H), 1644 (νC=O), 1532 (δN-H), 1281, 1134 (νC-F). MS (FAB$^+$, DTT/TG = 1/1) m/z 557 [M+H]$^+$. HRMS (positive ESI) Calcd for $C_{31}H_{27}F_6N_2O^+$ [M+H]$^+$: 557.2022. Found: 557.2046.

*1-Benzyl-4-hydroxy-5-oxo-N-trityl-2,5-dihydro-1H-pyrrole-3-carboxamide (**9a**)*

To a mixture of 3-(benzylamino)-*N*-tritylpropanamide (**8a**: 201 mg, 477 μmol) and diethyl oxalate (78.0 μl, 576 μmol) was added ethanolic sodium ethoxide, prepared by dissolving sodium (21.9 mg, 953 μmol) in dry ethanol (4 ml), and the mixture was stirring at 80 °C for 4h. After cooling to room temperature, the resulting precipitate was collected and then dissolved in water. The aqueous solution was acidified with 10% HCl to pH = 3. The resulting precipitate was collected and dried *in vacuo* to afford the aimed compound as a beige solid. (223 mg, 98%). Mp 186.5–1187.0 °C. ^{1}H NMR (400 MHz, $CDCl_3$) δ/ppm 3.92 (s, 2H), 4.62 (s, 2H), 7.18–7.33 (m, 20H), 8.26 (s, 1H). ^{13}C NMR (100 MHz, $CDCl_3$) δ/ppm 47.3, 47.5, 70.6, 114.9, 127.1, 128.1, 128.3, 128.5, 128.8, 129.1, 135.7, 144.9, 148.3, 161.6, 166.6. IR (KBr) ν_{max}/cm^{-1} 3384 (νN-H), 3032 (νO-H), 2638 (νC-H), 1668 (νC=O), 1521 (δN-H), 1240 (νC-O). HRMS (negative ESI) Calcd for $C_{31}H_{25}N_2O_3^-$ [M–H]$^-$: 473.1871. Found: 473.1901.

*4-Hydroxy-1-(4-methylbenzyl)-5-oxo-N-trityl-2,5-dihydro-1H-pyrrole-3-carboxamide (**9b**)*

To a mixture of 3-((4-methylbenzyl)amino)-*N*-tritylpropanamide (**8b**: 1.14 g, 2.61 mmol) and diethyl oxalate (425 μl, 3.14 mmol) was added ethanolic sodium ethoxide, prepared by dissolving sodium (120 mg, 5.22 mmol) in dry ethanol (30 ml), and the mixture was stirring at 80 °C for 2 days. After cooling to room temperature, the resulting precipitate was collected and then dissolved in water. The aqueous solution was acidified with 10% HCl to pH = 3. The resulting precipitate was collected and dried *in vacuo* to afford the aimed compound as a beige solid. (1.26 g, 99%). Mp 175.0–176.0 °C. ^{1}H NMR (400 MHz, $CDCl_3$) δ/ppm 2.33 (s, 3H), 3.88 (s, 2H), 4.58 (s, 2H), 7.12 (s, *4*H), 7.21–7.30 (m, 15H), 7.94 (br. s, 1H). ^{13}C NMR (100 MHz, $CDCl_3$) δ/ppm 21.3, 47.1, 47.2, 70.6, 114.9, 127.1, 128.0, 128.5, 128.8, 129.8, 132.7, 138.1, 144.9, 148.2, 161.6, 166.3. IR (KBr) ν_{max}/cm^{-1} 3526 (νN-H), 3367 (νO-H), 3056–2917 (νC-H), 1669 (νC=O), 1541 (δN-H), 1254 (νC-O). HRMS (negative ESI) Calcd for $C_{32}H_{27}N_2O_3^-$ [M–H]$^-$: 487.2027. Found: 487.2043.

*1-(4-Fluorobenzyl)-4-hydroxy-5-oxo-N-trityl-2,5-dihydro-1H-pyrrole-3-carboxamide (**9c**)*

To a mixture of 3-((4-fluorobenzyl)amino)-*N*-tritylpropanamide (**8c**: 1.17 g, 2.67 mmol) and diethyl oxalate (430 μl, 3.17 mmol) was added ethanolic sodium ethoxide, prepared by dissolving sodium (123 mg, 5.35 mmol) in dry ethanol (30 ml), and the mixture was stirring at 80 °C for 2 days. After cooling to room temperature, the resulting precipitate was collected and then dissolved in water. The aqueous solution was acidified with 10% HCl to pH = 3. The resulting precipitate was collected and dried *in vacuo* to afford the aimed compound as a beige solid. (1.24 g, 94%). Mp 167.5–168.5 °C. ^{1}H NMR (400 MHz, $CDCl_3$) δ/ppm 3.92 (s, 2H), 4.60 (s, 2H), 7.00 (t, *J* = 8.6 Hz, 2H), 7.18–7.29 (m, 17H), 8.25 (s, 1H), 10.42 (br. s, 1H). ^{13}C NMR (100 MHz, $CDCl_3$) δ/ppm 46.7, 47.3, 70.6, 115.3, 115.8 (d, $^2J_{CF}$ = 22 HZ), 127.1, 128.1, 128.8, 130.3 (d, $^3J_{CF}$ = 8 HZ), 131.6 (d, $^4J_{CF}$ = 4 HZ), 144.8, 147.9, 161.4, 162.7 (d, $^1J_{CF}$ = 248 HZ), 166.6. IR (KBr) ν_{max}/cm^{-1} 3518 (νN-H), 3364 (νO-H), 3060–2921 (νC-H), 1694, 1668 (νC=O), 1549 (δN-H), 1255 (νC-O). HRMS (negative ESI) Calcd for $C_{31}H_{24}FN_2O_3^-$ [M–H]$^-$: 491.1776. Found: 491.1755.

*1-(4-Chlorobenzyl)-4-hydroxy-5-oxo-N-trityl-2,5-dihydro-1H-pyrrole-3-carboxamide (**9d**)*

To a mixture of 3-((4-chlorobenzyl)amino)-*N*-tritylpropanamide (**8d**: 306 mg, 671 μmol) and diethyl oxalate (110 μl, 738 μmol) was added ethanolic sodium ethoxide, prepared by dissolving sodium (30.9 mg, 1.34 mmol) in dry ethanol (6 ml), and the mixture was stirring at 80 °C for 3h. After cooling to room temperature, the resulting precipitate was collected and then dissolved in water. The aqueous solution was acidified with 10% HCl to pH = 3. The resulting precipitate was collected and dried *in vacuo* to afford the aimed compound as a beige solid. (214 mg, 63%). Mp 184.2–184.5 °C. ^{1}H NMR (400 MHz, $CDCl_3$) δ/ppm 3.92 (s, 2H), 4.60 (s, 2H), 7.16 (d, *J* = 8.1 Hz, 2H), 7.23–7.29 (m, 17H), 8.16 (s, 1H), 10.11 (br. s, 1H). ^{13}C NMR (100 MHz, $CDCl_3$) δ/ppm 46.8, 47.3, 70.7, 115.0, 127.2, 128.1, 128.8, 129.3, 129.8, 134.2, 134.3, 144.8, 148.0, 161.5, 166.4. IR (KBr) ν_{max}/cm^{-1} 3527 (νN-H), 3392 (νO-H), 3025–2941 (νC-H), 1664 (νC=O), 1532 (δN-H), 1252 (νC-O). HRMS (negative ESI) Calcd for $C_{31}H_{24}ClN_2O_3^-$ [M–H]$^-$: 507.1481. Found: 507.1462.

*1-(3,5-Bis(trifluoromethyl)benzyl)-4-hydroxy-5-oxo-N-trityl-2,5-dihydro-1H-pyrrole-3-carboxamide (**9e**)*

To a mixture of 3-((3,5-bis(trifluoromethyl)benzyl)amino)-*N*-tritylpropanamide (**8e**: 354 mg, 6.36 μmol) and diethyl oxalate (100 μl, 738 μmol) was added ethanolic sodium ethoxide, prepared by dissolving sodium (29.2 mg, 1.27 mmol) in dry ethanol (6 ml), and the mixture was stirring at 80 °C for 16 h. After cooling to room temperature, the resulting precipitate was collected and then dissolved in water. The aqueous solution was acidified with 10% HCl to pH = 3. The resulting precipitate was collected and dried *in vacuo* to afford the aimed compound as a beige solid. (287 mg, 74%). Mp 178.0–178.8 °C. ^{1}H NMR (400 MHz, $CDCl_3$) δ/ppm 3.95 (s, 2H), 4.74 (s, 2H), 7.20–7.26 (m,

View Article Online
DOI: 10.1039/C7NJ00930D

15H), 7.68 (s, 2H), 7.85 (s, 1H), 8.24 (s, 1H), 10.20 (br. s, 1H). ^{13}C NMR (100 MHz, $CDCl_3$) δ/ppm 46.6, 47.5, 70.7, 115.8, 122.5 (q, $^3J_{CF}$ = 4 HZ), 123.1 (q, $^1J_{CF}$ = 274 HZ), 127.2, 128.1, 128.5 (q, $^3J_{CF}$ = 3 HZ), 128.7, 132.6 (q, $^2J_{CF}$ = 34 HZ), 138.4, 144.7, 147.6, 161.3, 166.8. IR (KBr) ν_{max}/cm^{-1} 3391 (νN-H), 2928-3060 (νO-H, νC-H), 1671 (νC=O), 1539 (δN-H), 1280 (νC-O), 1247, 1134 (νC-F). HRMS (negative ESI) Calcd for $C_{33}H_{23}F_6N_2O_3^-$ [M–H]$^-$: 609.1618. Found: 609.1614.

*1-Benzyl-4-hydroxy-5-oxo-2,5-dihydro-1H-pyrrole-3-carboxamide (**1a**)*

1-Benzyl-4-hydroxy-5-oxo-*N*-trityl-2,5-dihydro-1*H*-pyrrole-3-carboxamide (**9a**: 102 mg, 215 μmol) in 40% TFA in CH_2Cl_2 (2 ml) was stirried at r.t. for 30 min. The resulting solution was epaporated and washing with $CHCl_3$ to afford the product as a colorless solid (41.9 mg, 84%). Mp 214 °C (decomp.). ^{1}H NMR (400 MHz, DMSO-d_6) δ/ppm 3.80 (s, 2H), 4.59 (s, 2H), 6.95 (br, 1H), 7.22–7.38 (m, 5H), 7.45 (br, 1H). ^{13}C NMR (100 MHz, DMSO-d_6) δ/ppm 45.8, 46.0, 111.9, 127.5, 127.7, 128.7, 137.0, 150.8, 164.6, 165.0. IR (KBr) ν_{max}/cm^{-1} 3434 (ν_{as}N-H), 3158 (ν_sN-H), 1688, 1670 (νC=O), 1457 (νC-N), 1332, 1259 (νC-O). MS (FAB$^+$, DTT/TG = 1/1) m/z 233 [M+H]$^+$. Anal. Calcd. for $C_{12}H_{12}N_2O_3$: C, 62.06; H, 5.21; N, 12.06. Fond: C, 61.50; H, 5.09; N, 11.65.

*4-Hydroxy-1-(4-methylbenzyl)-5-oxo-2,5-dihydro-1H-pyrrole-3-carboxamide (**1b**)*

4-Hydroxy-1-(4-methylbenzyl)-5-oxo-*N*-trityl-2,5-dihydro-1*H*-pyrrole-3-carboxamide (**9b**: 102 mg, 208 μmol) in 40% TFA in CH_2Cl_2 (2 ml) was stirried at r.t. for 30 min. The resulting solution was epaporated and washing with $CHCl_3$ to afford the product as a colorless solid (35.7 mg, 70%). Mp 202 °C (decomp.). ^{1}H NMR (400 MHz, DMSO-d_6) δ/ppm 2.28 (s, 1H), 3.77 (s, 2H), 4.54 (s, 2H), 6.96 (br, 1H), 7.12 (d, *J* = 8.0 Hz, 2H), 7.17 (d, *J* = 8.0 Hz, 2H), 7.44 (br, 1H). ^{13}C NMR (100 MHz, DMSO-d_6) δ/ppm 20.7, 45.6, 45.8, 111.8, 127.8, 129.3, 133.9, 136.7, 150.9, 164.7, 164.9. IR (KBr) ν_{max}/cm^{-1} 3455 (ν_{as}N-H), 3196 (ν_sN-H), 2921 (νC-H), 1673, 1638 (νC=O), 1501 (νC-N), 1332, 1252 (νC-O). MS (FAB$^+$, DTT/TG = 1/1) m/z 247 [M+H]$^+$. Anal. Calcd. for $C_{13}H_{14}N_2O_3$: C, 63.40; H, 5.73; N, 11.38. Fond: C, 63.15; H, 5.69; N, 11.19.

*1-(4-Fluorobenzyl)-4-hydroxy-5-oxo-2,5-dihydro-1H-pyrrole-3-carboxamide (**1c**)*

1-(4-Fluorobenzyl)-4-hydroxy-5-oxo-*N*-trityl-2,5-dihydro-1*H*-pyrrole-3-carboxamide (**9c**: 74.2 mg, 151 μmol) in 40% TFA in CH_2Cl_2 (1.5 ml) was stirried at r.t. for 30 min. The resulting solution was epaporated and washing with $CHCl_3$ to afford the product as a colorless solid (22.8 mg, 60%). Mp 202 °C (decomp.). ^{1}H NMR (400 MHz, DMSO-d_6) δ/ppm 3.81 (s, 2H), 4.58 (s, 2H), 6.95 (br, 1H), 7.18 (td, *J* = 8.8, 3.0 Hz, 2H), 7.26–7.31 (m, 2H), 7.45 (br, 1H). ^{13}C NMR (100 MHz, DMSO-d_6) δ/ppm 45.1, 45.9, 112.0, 115.5 (d, $^2J_{CF}$ = 21 HZ). 129.9 (d, $^3J_{CF}$ = 8 HZ), 133.22 (d, $^4J_{CF}$ = 3 HZ), 150.7, 161.5 (d, $^1J_{CF}$ = 243 HZ), 164.6, 165.0. IR (KBr) ν_{max}/cm^{-1} 3476 (ν_{as}N-H), 3315 (ν_sN-H), 1682, 1634 (νC=O), 1501 (νC-N), 1337, 1252 (νC-O). MS (FAB$^+$, DTT/TG = 1/1) m/z 251 [M+H]$^+$. Anal. Calcd. for $C_{12}H_{11}FN_2O_3$: C, 57.60; H, 4.43; N, 11.20. Fond: C, 57.52; H, 4.39; N, 11.20.

*1-(4-Chlorobenzyl)-4-hydroxy-5-oxo-2,5-dihydro-1H-pyrrole-3-carboxamide (**1d**)*

1-(4-Chlorobenzyl)-4-hydroxy-5-oxo-*N*-trityl-2,5-dihydro-1*H*-pyrrole-3-carboxamide (**9d**: 119 mg, 234 μmol) in 40% TFA in CH_2Cl_2 (2 ml) was stirried at r.t. for 30 min. The resulting solution was epaporated and washing with $CHCl_3$ to afford the product as a colorless solid (41.6 mg, 67%). Mp 212 °C (decomp.). ^{1}H NMR (400 MHz, DMSO-d_6) δ/ppm 3.82 (s, 2H), 4.58 (s, 2H), 6.97 (br, 1H), 7.26 (d, *J* = 8.4 Hz, 2H), 7.42 (d, *J* = 8.4 Hz, 2H), 7.48 (br, 1H). ^{13}C NMR (100 MHz, DMSO-d_6) δ/ppm 45.2, 46.1, 112.1, 128.7, 129.6, 132.1, 136.1, 150.7, 164.6, 165.1. IR (KBr) ν_{max}/cm^{-1} 3464 (ν_{as}N-H), 3334 (ν_sN-H), 1694, 1672 (νC=O), 1456 (νC-N), 1325, 1251 (νC-O). MS (FAB$^+$, DTT/TG = 1/1) m/z 267 [M+H]$^+$. Anal. Calcd. for $C_{12}H_{11}ClN_2O_3$: C, 54.05; H, 4.16; N, 10.50. Fond: C, 53.85; H, 4.07; N, 10.59.

*1-(3,5-Bis(trifluoromethyl)benzyl)-4-hydroxy-5-oxo-2,5-dihydro-1H-pyrrole-3-carboxamide (**1e**)*

1-(3,5-Bis(trifluoromethyl)benzyl)-4-hydroxy-5-oxo-*N*-trityl-2,5-dihydro-1*H*-pyrrole-3-carboxamide (**9e**: 119 mg, 234 μmol) in 40% TFA in CH_2Cl_2 (2 ml) was stirried at r.t. for 30 min. The resulting solution was epaporated and washing with $CHCl_3$ to afford the product as a colorless solid (34.1 mg, 47%). Mp 212 °C (decomp.). ^{1}H NMR (400 MHz, DMSO-d_6) δ/ppm 3.92 (s, 2H), 4.78 (s, 2H), 6.96 (br, 1H), 7.47 (br, 1H) 7.96 (s, 2H), 8.05 (s, 1H). ^{13}C NMR (100 MHz, DMSO-d_6) δ/ppm 45.3, 46.6, 112.7, 121.4 (q, $^3J_{CF}$ = 4 HZ), 123.3 (q, $^1J_{CF}$ = 273 HZ), 128.8 (q, $^3J_{CF}$ = 3 HZ), 130.5 (q, $^2J_{CF}$ = 33 HZ), 141.0, 150.7, 164.8, 165.8. IR (KBr) ν_{max}/cm^{-1} 3461 (ν_{as}N-H), 3307 (ν_sN-H), 1684 (νC=O), 1382 (νC-N), 1282 (νC-F), 1173, 1129 (νC-O). MS (FAB$^+$, DTT/TG = 1/1) m/z 369 [M+H]$^+$. Anal. Calcd. for $C_{14}H_{10}F_6N_2O_3$: C, 45.66; H, 2.74; N, 7.61. Fond: C, 44.87; H, 3.21; N, 7.65.

*Bis(1-benzyl-3-carbamoyl-2,5-dihydro-5-oxo-1H-pyrrol-4-olato)zinc(II) (**10a**)*

1-Benzyl-4-hydroxy-5-oxo-2,5-dihydro-1*H*-pyrrole-3-carboxamide (**1a**: 107 mg, 462 μmol) and lithium hydroxide monohydrate (33.5 mg, 798 μmol) were dissolved in water/THF mixture solution (1:1, 4 ml), and then 1M $ZnSO_4$ aq. (220 μl, 220 μmol) was added to the solution. The mixture was stirred for 2 hours. The resulting precipitate was collected by suction filtration, and dried *in vacuo* to afford the aimed compound as a colorless solid (91.4 mg, 79%). ^{1}H NMR (400 MHz, DMSO-d_6) δ/ppm 3.75 (s, 4H), 4.62 (s, 4H), 7.19–7.23 (m, 4H), 7.26–7.39 (m, 6H). IR (KBr) ν_{max}/cm^{-1} 3397 (ν_{as}N-H), 3208 (ν_sN-H), 1655, 1624 (νC=O), 1339, 1261 (νC-O). Anal. Calcd. for $C_{24}H_{22}N_4O_6Zn \bullet 2.0H_2O$: C, 51.12; H, 4.65; N, 9.94. Fond: C, 51.04; H, 4.62; N, 9.64.

*Bis{3-Carbamoyl-2,5-dihydro-1-(4-methylbenzyl)-5-oxo-1H-pyrrol-4-olato}zinc(II) (**10b**)*

4-Hydroxy-1-(4-methylbenzyl)-5-oxo-2,5-dihydro-1*H*-pyrrole-3-carboxamide (**1b**: 83.7 mg, 340 μmol) and lithium hydroxide monohydrate (23.6 mg, 562 μmol) were dissolved in water/THF mixture solution (1:1, 3 ml), and then 1M $ZnSO_4$ aq. (170 μl, 170 μmol) was added to the solution. The mixture was stirred for 2

hours. The resulting precipitate was collected by suction filtration, and dried *in vacuo* to afford the aimed compound as a colorless solid (99.4 mg, quant.). ^{1}H NMR (400 MHz, DMSO-d_6) δ/ppm 2.28 (s, 6H), 3.73 (s, 4H), 4.56 (s, 4H), 7.10 (d, J = 7.8 Hz, 4H), 7.16 (d, J = 7.8 Hz, 4H). IR (KBr) ν_{max}/cm^{-1} 3399 (ν_{as}N-H), 3220 (ν_sN-H), 1655, 1625 (νC=O), 1336, 1260 (νC-O). Anal. Calcd. for $C_{26}H_{26}N_4O_6Zn\bullet1.2H_2O$: C, 54.07; H, 4.96; N, 9.70. Fond: C, 54.16; H, 4.89; N, 9.64.

*Bis{3-Carbamoyl-1-(4-fluorobenzyl)-2,5-dihydro-5-oxo-1H-pyrrol-4-olato}zinc(II) (**10c**)*

1-(4-Fluorobenzyl)-4-hydroxy-5-oxo-2,5-dihydro-1*H*-pyrrole-3-carboxamide (**1c**: 86.7 mg, 346 µmol) and lithium hydroxide monohydrate (17.8 mg, 424 µmol) were dissolved in water/THF mixture solution (1:1, 3 ml), and then 1M $ZnSO_4$ aq. (170 µl, 170 µmol) was added to the solution. The mixture was stirred for 2 hours. The resulting precipitate was collected by suction filtration, and dried *in vacuo* to afford the aimed compound as a colorless solid (95.6 mg, 97%). ^{1}H NMR (400 MHz, DMSO-d_6) δ/ppm 3.75 (s, 4H), 4.60 (s, 4H), 7.15–7.21 (m, 4H), 7.23–7.29 (m, 4H). IR (KBr) ν_{max}/cm^{-1} 3399 (ν_{as}N-H), 3216 (ν_sN-H), 1651, 1624 (νC=O), 1337, 1261 (νC-O). Anal. Calcd. for $C_{24}H_{20}F_2N_4O_6Zn\bullet1.8H_2O$: C, 48.35; H, 3.99; N, 9.40. Fond: C, 48.29; H, 4.16; N, 9.23.

*Bis{3-carbamoyl-1-(4-chlorobenzyl)-2,5-dihydro-5-oxo-1H-pyrrol-4-olato}zinc(II) (**10d**)*

1-(4-Chlorobenzyl)-4-hydroxy-5-oxo-2,5-dihydro-1*H*-pyrrole-3-carboxamide (**1d**: 73.7 mg, 276 µmol) and lithium hydroxide monohydrate (27.6 mg, 657 µmol) were dissolved in water/THF mixture solution (1:1, 3 ml), and then 1M $ZnSO_4$ aq. (140 µl, 140 µmol) was added to the solution. The mixture was stirred for 2 hours. The resulting precipitate was collected by suction filtration, and dried *in vacuo* to afford the aimed compound as a colorless solid (58.0 mg, 70%). ^{1}H NMR (400 MHz, DMSO-d_6) δ/ppm 3.75 (s, 4H), 4.61 (s, 4H), 7.23 (d, J = 8.2 Hz, 4H), 7.41 (d, J = 8.2 Hz, 4H) . IR (KBr) ν_{max}/cm^{-1} 3398 (ν_{as}N-H), 3216 (ν_sN-H), 1651, 1625 (νC=O), 1338, 1262 (νC-O). Anal. Calcd. for $C_{24}H_{20}Cl_2N_4O_6Zn\bullet1.5H_2O$: C, 46.21; H, 3.72; N, 8.98. Fond: C, 46.27; H, 3.81; N, 8.61.

*Bis{1-(3,5-bis(trifluoromethyl)benzyl)-3-carbamoyl-2,5-dihydro-5-oxo-1H-pyrrol-4-olato}zinc(II) (**10e**)*

1-(3,5-Bis(trifluoromethyl)benzyl)-4-hydroxy-5-oxo-2,5-dihydro-1*H*-pyrrole-3-carboxamide (**1e**: 97.1 mg, 264 µmol) and lithium hydroxide monohydrate (23.6 mg, 562 µmol) were dissolved in water/THF mixture solution (1:1, 4 ml), and then 1M $ZnSO_4$ aq. (130 µl, 130 µmol) was added to the solution. The mixture was stirred for 3 hours. The resulting precipitate was collected by suction filtration, and dried *in vacuo* to afford the aimed compound as a colorless solid (173 mg, quant.). ^{1}H NMR (400 MHz, DMSO-d_6) δ/ppm 3.82 (s, 4H), 4.80 (s, 4H), 7.90 (s, 4H), 8.06 (s, 2H). IR (KBr) ν_{max}/cm^{-1} 3451 (ν_{as}N-H), 3343(ν_sN-H), 1652, 1634 (νC=O), 1281 (νC-F), 1176, 1131 (νC-O). Anal. Calcd. for $C_{28}H_{18}F_{12}N_4O_6Zn\bullet0.5H_2O$: C, 41.58; H, 2.37; N, 6.93. Fond: C, 41.54; H, 2.65; N, 6.78.

Molecular docking

View Article Online
DOI: 10.1039/C7NJ00370D

The optimized structures and atomic charges of the selected ligands were estimated using the semi-empirical PM7 calculation method,[36] prior to conducting docking simulations. All docking experiments were carried out using GOLD Suite software package (ver. 5.2) obtained from the Cambridge Crystallographic Data Centre (CCDC).[37] ChemPLP scoring function[38] was used for pose prediction, and the obtained poses were rescored using GOLDscore.[39] The best pose for each ligand was determined by considering the results obtained using both scoring functions. All docking results were visualized by Hermes software package (ver. 1.6) provided by CCDC.[40] All calculations were conducted using a PC with an Intel Core™ i3-3220 processor (3.30 GHz) and 8GB RAM.

***In vitro* insulin-mimetic activity**[16, 17]

Male Wistar rats were sacrificed under anesthesia with ether. The adipose tissues were removed, chopped with scissors, and digested with collagenase for 60 min at 37 °C in Krebs-Ringer bicarbonate buffer (120 mM NaCl, 1.27 mM $CaCl_2$, 1.2 mM $MgSO_4$, 4.75 mM KCl, 1.2 mM KH_2PO_4, 24 mM $NaHCO_3$, pH 7.4) containing 2% bovine serum albumin. The adipocytes were then separated from the undigested tissues and washed with buffer three times. The isolated adipocyte solutions were pre-incubated at 37 °C for 30 min with various concentrations of the zinc(II) complexes or $ZnSO_4$ in saline containing 5 mM glucose. Then, a solution of epinephrine was added to the reaction mixtures (final concentration: 10 mM) and the resulting solutions were incubated at 37 °C for 3 h. The reaction was stopped by soaking in ice water and the mixtures were centrifuged at 3000 rpm (600 *g*) at 4 °C for 10 min. The level of FFA in the extracellular fluid was determined using an FFA kit (NEFA C-test Wako, Wako Pure Chemicals, Osaka, Japan).

All animal experiments were approved by the Experimental Animal Research of Kyoto Pharmaceutical University (KPU) and were performed according to the Guideline for Animal Experimentation of KPU.

Notes and references

1. L. Stryer, *Biochemistry*, W. H. Freeman and Company, New York, 3rd edn., 1988.
2. WHO, *World Health Organ. Tech. Rep. Ser.*, 1985, **727**, 1-113.
3. A. F. Amos, D. J. McCarty and P. Zimmet, *Diabetic Med.*, 1997, **14**, S7-S85.
4. E. Standl and M. Fuchtenbusch, *Diabetologia*, 2003, **46**, M30-M36.
5. M. Brownlee, *Nature*, 2001, **414**, 813-820.
6. Z. Changjin, in *Diabetes Mellitus - Insights and Perspectives*, ed. O. Oguntibeju, InTech, 2013, DOI: 10.5772/54642, ch. 2, pp. 17-46.
7. M. Lorenzi, *Exp. Diabetes Res.*, 2007, DOI: Doi 10.1155/2007/61038, Article ID 61038, 61010 pages.
8. N. Hotta, *Biomed. Pharmacother.*, 1995, **49**, 232-243.
9. L. Costantino, G. Rastelli, P. Vianello, G. Cignarella and D. Barlocco, *Med. Res. Rev.*, 1999, **19**, 3-23.
10. H. Sakurai, Y. Kojima, Y. Yoshikawa, K. Kawabe and H. Yasui,

Coord. Chem. Rev., 2002, **226**, 187-198.
11. A. Shisheva, D. Gefel and Y. Shechter, *Diabetes*, 1992, **41**, 982-988.
12. M. D. Chen, S. J. Liou, P. Y. Lin, V. C. Yang, P. S. Alexander and W. H. Lin, *Biol. Trace Elem. Res.*, 1998, **61**, 303-311.
13. A. Nazarizadeh and S. Asri-Rezaie, *AAPS PharmSciTech*, 2016, **17**, 834-843.
14. M. Yamaguchi, K. Wakasugi, R. Saito, Y. Adachi, Y. Yoshikawa, H. Sakurai and A. Katoh, *J. Inorg. Biochem.*, 2006, **100**, 260-269.
15. M. Yamaguchi, R. Saito, Y. Adachi, Y. Yoshikawa, H. Sakurai and A. Katoh, *Heterocycles*, 2007, **73**, 603-615.
16. Y. Yoshikawa and H. Yasui, *Curr. Top. Med. Chem.*, 2012, **12**, 210-218.
17. K. Vijayaraghavan, S. I. Pillai and S. P. Subramanian, *Eur. J. Pharmacol.*, 2012, **680**, 122-129.
18. S. Fujimoto, H. Yasui and Y. Yoshikawa, *J. Inorg. Biochem.*, 2013, **121**, 10-15.
19. S. Kadowaki, M. Munekane, Y. Kitamura, M. Hiromura, S. Kamino, Y. Yoshikawa, H. Saji and S. Enomoto, *Biol. Trace Elem. Res.*, 2013, **154**, 111-119.
20. M. E. Lopez-Viseras, B. Fernandez, S. Hilfiker, C. S. Gonzalez, J. L. Gonzalez, A. J. Calahorro, E. Colacio and A. Rodriguez-Dieguez, *J. Inorg. Biochem.*, 2014, **131**, 64-67.
21. T. Kolesa-Dobravc, K. Maejima, Y. Yoshikawa, A. Meden, H. Yasui and F. Perdih, *New J. Chem.*, 2017, **41**, 735-746.
22. H. Kawarada, Y. Yoshikawa, H. Yasui, S. Kuwahara, Y. Habata and R. Saito, *Metallomics*, 2011, **3**, 675-679.
23. B. L. Mylari, T. A. Beyer and T. W. Siegel, *J. Med. Chem.*, 1991, **34**, 1011-1018.
24. H. Murakami, H. Yasui and Y. Yoshikawa, *Chem. Pharm. Bull.*, 2012, **60**, 1096-1104.
25. D. R. Reddy, M. A. Iqbal, R. L. Hudkins, P. A. Messina-McLaughlin and J. P. Mallamo, *Tetrahedron Lett.*, 2002, **43**, 8063-8066.
26. M. C. Rodriguez-Arguelles, S. Mosquera-Vazquez, J. Sanmartin-Matalobos, A. M. Garcia-Deibe, C. Pelizzi and F. Zani, *Polyhedron*, 2010, **29**, 864-870.
27. A. S. Smirnov, E. S. Butukhanova, N. A. Bokach, G. L. Starova, V. V. Gurzhiy, M. L. Kuznetsov and V. Y. Kukushkin, *Dalton Trans.*, 2014, **43**, 15798-15811.
28. R. Saito, M. Tokita, K. Uda, C. Ishikawa and M. Satoh, *Tetrahedron*, 2009, **65**, 3019-3026.
29. A. Del Corso, L. Costantino, G. Rastelli, F. Buono and U. Mura, *Exp. Eye Res.*, 2000, **71**, 515-521.
30. C. A. Sotriffer, O. Kramer and G. Klebe, *Proteins*, 2004, **56**, 52-66.
31. H. Steuber, M. Zentgraf, C. La Motta, S. Sartini, A. Heine and G. Klebe, *J. Mol. Biol.*, 2007, **369**, 186-197.
32. R. Maccari, R. Ottana, R. Ciurleo, D. Rakowitz, B. Matuszczak, C. Laggner and T. Langer, *Bioorg. Med. Chem.*, 2008, **16**, 5840-5852.
33. X. Chen, C. Zhu, F. Guo, X. Qiu, Y. Yang, S. Zhang, M. He, S. Parveen, C. Jing, Y. Li and B. Ma, *J. Med. Chem.*, 2010, **53**, 8330-8344.
34. D. H. Harrison, K. M. Bohren, D. Ringe, G. A. Petsko and K. H. Gabbay, *Biochemistry*, 1994, **33**, 2011-2020.
35. M. Nakai, H. Watanabe, C. Fujiwara, H. Kakegawa, T. Satoh, J. Takada, R. Matsushita and H. Sakurai, *Biol Pharm Bull*, 1995, **18**, 719-725.
36. J. J. P. Stewart, *J. Mol. Model.*, 2013, **19**, 1-32.
37. G. Jones, GOLD (Version 5.2), The Cambridge Crystallographic Data Centre (CCDC), Cambridge, UK.
38. O. Korb, T. Stützle and T. E. Exner, *J. Chem. Inf. Model.*, 2009, **49**, 84-96.
39. M. L. Verdonk, J. C. Cole, M. J. Hartshorn, C. W. Murray and R. D. Taylor, *Proteins*, 2003, **52**, 609-623.
40. Hermes (Version 1.6), The Cambridge Crystallographic Data Centre (CCDC), Cambridge, UK.